Hindawi
International Transactions on Electrical Energy Systems
Volume 2022, Article ID 1727524, 17 pages
https://doi.org/10.1155/2022/1727524

*Research Article*

# Optimal Energy Management of Virtual Power Plants with Storage Devices Using Teaching-and-Learning-Based Optimization Algorithm

**Raji Krishna and S. Hemamalini**

*School of Electrical Engineering, Vellore Institute of Technology, Chennai, Tamil Nadu 600127, India*

Correspondence should be addressed to S. Hemamalini; hemamalini.s@vit.ac.in

Received 6 January 2022; Revised 29 May 2022; Accepted 15 June 2022; Published 29 August 2022

Academic Editor: Jaouher Ben Ali



In recent decades, Renewable Energy Sources (RES) have become more attractive due to the depleting fossil fuel resources and environmental issues such as global warming due to emissions from fossil fuel-based power plants. However, the intermittent nature of RES may cause a power imbalance between the generation and the demand. The power imbalance is overcome with the help of Distributed Generators (DG), storage devices, and RES. The aggregation of DGs, storage devices, and controllable loads that form a single virtual entity is called a Virtual Power Plant (VPP). In this article, the optimal scheduling of DGs in a VPP is done to minimize the generation cost. The optimal scheduling of power is done by exchanging the power between the utility grid and the VPP with the help of storage devices based on the bidding price. In this work, the state of charge (SOC) of the batteries is also considered, which is a limiting factor for charging and discharging of the batteries. This improves the lifetime of the batteries and their performance. Energy management of VPP using the teaching-and-learning-based optimization algorithm (TLBO) is proposed to minimize the total operating cost of VPP for 24 hours of the day. The power loss in the VPP is also considered in this work. The proposed methodology is validated for the IEEE 16-bus and IEEE 33-bus test systems for four different cases. The results are compared with other evolutionary algorithms, like Artificial Bee Colony (ABC) algorithm and Ant Lion Optimization (ALO) algorithm.

## 1. Introduction

An increase in power demand and restrictions imposed on fossil fuel usage to reduce power plant emissions have made utilities look for alternate sources. Also, power distribution to remote locations is still a problem due to technical and financial issues. To mitigate these problems, distributed generators like wind, solar, fuel cells, and so on are used. The government also announces useful schemes and policies such as Renewable Portfolio Standards (RPS) and different kinds of subsidies at different levels to encourage the usage of renewable energy sources for power generation. The global power generation [1] using wind and solar energy has increased to 743 GW and 874 GW at the end of 2021, with an 8% growth in renewable capacity.

Consumers need electrical energy at a cheaper cost, with high reliability and high quality. VPP is one of the remarkable solutions [2] to enhance power quality and reliability. VPP is a small, single imaginary power plant consisting of distributed generators (DGs), energy storage devices, and controllable loads along with information and communication technologies that plan, monitor the operation and coordinate the power flow between the components. Distributed generators consist of clean energy sources such as photovoltaic (PV), wind, Micro Turbines (MT), Fuel Cells (FC), diesel generators, and Combined Heat Power Plants (CHPP). In VPP, the storage devices (battery, electric vehicle, and battery-based robots) play a major role in energy exchange between the utility grid and VPP [3]. There are two types of VPP: commercial VPP and technical VPP. VPPs minimize the generation costs, minimize emissions, maximize profit, and enhance the trade in the electricity market. One of the main advantages of VPP is the integration of RES, which helps to reduce the deviation from the predicted generation

of electricity and associated penalties. The other advantage is the integration of EVs, which can act as a storage device in the power system [4].

Even though RES helps to reduce the emission, RES is not sufficient to meet the power demand and may fail to maintain the power balance between the generation and the load demand during peak hours. This problem can be overcome in VPPs, wherein the power generation from other distributed resources and storage devices along with power generated from RES maintains the power balance [3]. During peak load, VPP can support the grid by supplying its reserves. Likewise, when the pricing of utility power is lesser than that of the VPP, VPP buys power from the utility grid. Optimal scheduling of each unit in a VPP is thereby important for the economical operation. Various optimization techniques are used for the optimal operation of VPP [5, 6]. For proper functioning of VPP, the Energy Management System (EMS) is responsible for controlling the flow of power between the generating units, controllable loads, and the storage devices. There are various challenges associated with EMS of VPP, such as uncertainty of Renewable Energy Sources (RES), market price, power balancing, and integration of all the units in VPP [7, 8].

Energy management in a VPP is done by replacing the diesel generators with RESs and energy storage devices [9]. The proper balance between the power generation and the load demand is essential to avoid the instability problems in the VPP operation. DG, being the peak load provider during peak hours, helps to maintain the power balance between power generation and consumption [10]. The penetration of various DGs, especially the RES, will bring more uncertainties in the power system operation. Various mathematical methods are used in the literature to model the uncertainty of RES. A Probabilistic Load Flow (PLF) using the unscented transformation (UT) method is introduced in [11] to analyze the system performance. The increased utilization of PEVs along with the high penetration of RES will affect the optimal operation of the distribution feeder reconfiguration (DFR) strategy in the smart grids. To mitigate this problem and to increase the efficiency of the system, the V2G concept is proposed and the uncertainty of RES is modeled with the UT method [12]. The robust optimization model is used for calculating the generation cost of VPP on an hourly basis that is proposed in [13–16] while considering the uncertainty of PV and wind. A two-stage Stackelberg game is proposed for the day-ahead energy management of VPP considering the uncertainty of RES and market price [17]. A combination of Stochastic Programming and Adaptive Robust Optimization (ARO) based approach is proposed to model the uncertainty of market price [18]. Integration of Electric vehicles (EVs) is a new trend for power balancing in VPP. Integrating more and more uncertain sources of energy such as PV, wind, and energy storage devices makes the system highly dynamic. Thereby, to maximize the profit of a VPP, Hybrid Levy Particle Swarm Variable Neighborhood Search Optimization (HL-PS-VNSO) [19] is suggested. The uncertainties due to plug-in-electric vehicles (PHEVs) in G2V (additional load to the grid) and market price are also considered.

Energy storage devices play a vital role in maintaining the power balance in a VPP by selling or buying the power from the VPP [20]. Energy storage devices, like fuel cells and batteries, supply power to additional or instantaneous loads. Regulation of SOC of battery is an important aspect to enhance the proper power flow between the utility grid and the VPP. A fuzzy-based control strategy [21] is applied for the regulation of SOC and for controlling the power flow during excess and insufficient conditions. The concept of electric vehicles (EVs) to store energy to overcome the intermittent supply of energy from the wind farms is discussed in [22].

The metaheuristic techniques reduce computational time compared with conventional methods [23]. Dimeas and Hatziargyriou used Multiagent System- (MAS-) based control [24] for the optimal and effective control of a VPP. It is claimed that in centralized systems, MAS provides a better solution, but not an optimal solution. De Filippo et al. introduced a two-stage optimization model [25] for a VPP EMS, which decides the optimal planning of power flows for each time step at minimum cost. In this two-stage model, in the first stage, the prediction of uncertainty is modeled using a robust approach to optimize the load demand shift and estimate the cost. In the second stage, an online greedy optimization algorithm is implemented within the simulator that uses the optimal shift produced in the first stage to minimize the operating cost. However, there is a loss of quality in the solution because of the greedy algorithm used in the second step.

The minimization of the total cost and thereby maximation of the profit is the major concept associated with VPP. Profit maximization of VPP in a day-ahead market taking into account the uncertainty of RES is proposed [26]. The bidding strategy for a VPP is formulated as an optimization problem to maximize the profit using MILP. To reduce the operating cost while maintaining energy balance, system security, and system voltage level, a two-stage stochastic optimization model is introduced to address the uncertainties in the wind power outputs and electricity prices [27]. Results validated the reduction in operating costs while maintaining system reliability. An economic dispatch of VPP modeled using mixed-integer programming is presented in [28]. Bilevel mathematical programming used to model the bidding strategy is proposed [29] to maximize the profit and minimize the emission of VPPs. Computational intelligence- (CI-) based metaheuristic techniques [30] are increasingly used for profit maximization in VPPs. A trading model [31] of a VPP in a unified market is proposed and solved using the fruit fly algorithm (FFA) to maximize the profit.

However, most of these optimization techniques require algorithm parameters that need to be tuned to improve the performance of the techniques. Also, CI-based metaheuristic methods are not efficient to handle uncertainty in real-time situations. All these disadvantages can be overcome using the TLBO algorithm. In addition, the TLBO algorithm does not require any parameter to be tuned, which makes the implementation of TLBO much simpler.

In this paper, minimization of the operational cost of a commercial VPP for 24 hours in a day is formulated as the

optimization problem. Power losses are also taken into account. The VPP consists of solar, wind, MT, FC, and battery as energy sources. VPP can supply or buy power from the utility grid depending upon the cost of power generation and load demand in the VPP and the utility price. Though there are many techniques available in the literature to solve this problem, in this paper, the TLBO algorithm is used to solve the cost minimization problem by considering 4 different scenarios. Since the operating cost of RES is less compared to other generating units in the VPP, power output from the RES is utilized to the maximum. The optimal dispatch of generating units considering the power losses in the distribution system is done using backward-forward sweep load flow analysis. SOC of batteries is also taken into account, which enhances the battery life and its performance.

This paper is organized as follows. In Section 2, the basic structure of EMS for VPP, problem formulation, and the related constraints are discussed. An overview of the TLBO algorithm is presented in Section 3. In Section 4, the implementation of the TLBO algorithm for energy management in VPP is presented. Section 5 discusses the simulation results of 4 different cases and their comparison with ABC and ALO algorithms. Finally, the conclusion and future scope are discussed in Section 6.

## 2. Optimal Energy Management of Virtual Power Plants

The objective of a VPP is to relieve the load on the grid by smartly distributing the power generated by the individual units during peak load. A VPP and its components connected to a utility grid is represented in Figure 1. The main functionality of the EMS is to ensure proper power exchange between the utility grid and the VPP through proper coordination between the DGs and the grid. Energy is exchanged between the VPP and utility grid and thereby trading is done. This in turn can minimize the total operating cost or maximize the profit of a VPP. The EMS continuously monitors the status of each unit and sends suitable control signals to control the operation of DGs, energy storage devices, and controllable loads in an economical manner.

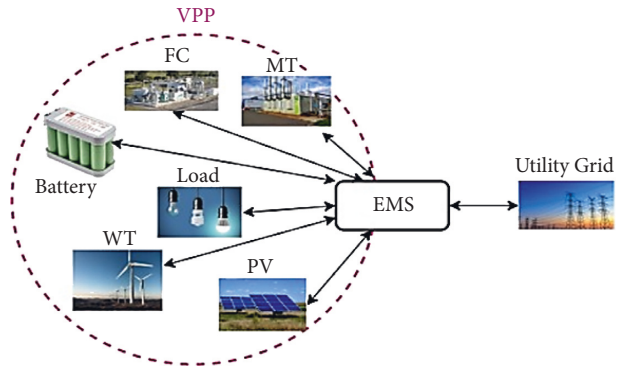


Figure 1: A virtual power plant (VPP) connected to a utility grid.

*2.1. Problem Formulation.* The main objective of the proposed work is the optimal allocation of generating units and the storage devices to minimize the operational cost of VPP in 24 hours of a day using the TLBO algorithm. In addition, the operating limits of the storage device, say the battery, are also considered in this work. The SOC of the battery is set to operate in the range of 10% to 90% of the battery capacity. This will improve the performance and lifetime of the storage device. Depending upon the load demand and the price of generation, power can either be sold or purchased from the main grid. Considering the hourly basis of usage, if the per-unit cost of the utility grid is less than the cost of VPP power, buying the power from the utility grid is economical. The power bought from the utility grid is also stored in the storage devices. On the other hand, if the utility price is more, then power from the VPP is sold to the utility. The objective function of the VPP is formulated to include the cost of power purchase from the utility grid, the fuel cost of the DGs and storage devices, and the start-up/shutdown cost of the power sources in the VPP [32]. In addition, the cost of power losses is also taken into account. Power losses are calculated using the forward-backward sweep method [33].

The objective function for the problem statement mentioned above is given as follows.

$$\text{Min}\left(f\left(X\right)\right) = \sum_{t=1}^{N_T} \left\{ \begin{array}{c} P_{\text{WT}}^t \times U_{\text{WT}}^t \times C_{\text{WT}}^t + P_{\text{PV}}^t \times U_{\text{PV}}^t \times C_{\text{PV}}^t + \\ P_{\text{FC}}^t \times U_{\text{FC}}^t \times C_{\text{FC}}^t + P_{\text{MT}}^t \times U_{\text{MT}}^t \times C_{\text{MT}}^t \\ + \sum_{i=1}^{N_g} S_{Gi}\left(U_i^t - U_i^{t-1}\right) + U_{\text{ESS}}^t \times P_{\text{ESS}}^t \times C_{\text{ESS}}^t \\ + \sum_{j=1}^{N_s} S_{sj}\left(U_j^t - U_j^{t-1}\right) + P_{\text{Grid}}^t \times C_{\text{Grid}}^t - P_{\text{Losses}}^t \times C_{\text{Losses}}^t \end{array} \right\}, \tag{1}$$

where $P_{\text{Losses}} = \sum_{k=1}^{M} (I_k)^2 R_k$.

$$\mathbf{I_k} = \left(\frac{\mathbf{P_i} + \mathbf{jQ_i}}{\mathbf{V_i}}\right)^*, \tag{2}$$

where $I_k$ is the current flow in the $k$th branch, $R_k$ is the resistance of the $k$th branch, and $M$ is the number of feeder sections/branches. $P^t_{\mathrm{PV}}, P^t_{\mathrm{WT}}, P^t_{\mathrm{FC}}, P^t_{\mathrm{MT}}, P^t_{\mathrm{ESS}}, P^t_{\mathrm{Grid}}$, and $P^t_{\mathrm{Losses}}$ are the available power from the PV, wind, turbine, fuel cell, microturbine, storage devices, utility grid, and power losses, respectively. $C^t_{\mathrm{PV}}, C^t_{\mathrm{WT}}, C^t_{\mathrm{FC}}, C^t_{\mathrm{MT}}, C^t_{\mathrm{ESS}}$, and $C^t_{\mathrm{Grid}}$ are the bidding price of the PV, wind turbine, fuel cell, microturbine, storage devices, and utility grid, respectively. $C^t_{\mathrm{Losses}}$ is the cost incurred towards the power losses. The ON/OFF status of all the corresponding units is represented by $U^t_{\mathrm{PV}}, U^t_{\mathrm{WT}}, U^t_{\mathrm{FC}}, U^t_{\mathrm{MT}}$, and $U^t_{\mathrm{ESS}}$. The start-up or shutdown costs for the $i$th DGs and $j$th storage devices are given as $S_{Gi}(t)$and $S_{sj}(t)$, respectively. $N_g$ and $N_s$ are the numbers of distributed generators and the storage units, respectively. $U^t_i$and $U^{t-1}_i$ are the ON/OFF status of DG units and $U^t_j$and $U^{t-1}_j$ are the ON/OFF status of storage devices with respect to time $t$ and $t-1$, respectively.

*2.2. Constraints.* At any given time, the power generation and the load demand in the VPP must be balanced; that is, the total power generation must equal the sum of load demand and losses as expressed in

$$\sum_{i=1}^{Ng} P_{Gi} + \sum_{j=1}^{Ns} P_{Sj} + P_{\mathrm{Grid}} = \sum_{k=1}^{N_{\mathrm{Load}}} P_{\mathrm{Load},k} + P_{\mathrm{Losses}}, \tag{3}$$

where $N_g$, $N_s$, and $N_{\mathrm{load}}$ are the numbers of distributed generators, the storage units, and loads, respectively.

The power generation limits of DGs, storage devices, and utility grid are expressed as

$$\begin{aligned} P_{Gi,\min} \le P_{Gi} \le P_{Gi,\max}, \\ P_{Sj,\min} \le P_{Sj} \le P_{Sj,\max}, \\ P_{\mathrm{Grid},\min} \le P_{\mathrm{Grid}} \le P_{\mathrm{Grid},\max}, \end{aligned} \tag{4}$$

where $P_{Gi,\min}$ and $P_{Gi,\max}$ are the minimum and maximum allowable powers of DGs, $P_{Sj,\min}$ and $P_{Sj,\max}$ are the minimum and maximum allowable power of the storage devices, and $P_{\mathrm{Grid},\min}$ and $P_{\mathrm{Grid},\max}$ are the minimum and maximum allowable powers of the utility grid. $P_{Gi}, P_{Sj}$, and $P_{\mathrm{Grid}}$ are the available power from the DGs, storage devices, and utility grid, respectively. The state of charge of the storage device is expressed as

$$\begin{aligned} SOC_{\mathrm{ESS}}(t) = SOC_{\mathrm{ESS}}(t-1) + \eta_{\mathrm{Charge}} P_{\mathrm{Charge}}(t)\Delta t \\ - \eta_{\mathrm{Discharge}} P_{\mathrm{Discharge}}(t)\Delta t, \quad t = 1,2,\ldots T, \end{aligned} \tag{5}$$

Where $SOC_{Ess}(t)$ and $SOC_{Ess}(t-1)$ are the energy stored in the devices at time $t$ and $t-1$, respectively. $P_{\mathrm{Charge}}$ and $P_{\mathrm{Discharge}}$ are the charging and discharging power at an instant, $\Delta t$ is a definite time, and $\eta_{\mathrm{Charge}}$ and $\eta_{\mathrm{Discharge}}$ are the efficiency during charging and discharging. The SOC, charging, and discharging limits of the storage devices are expressed as

$$SOC_{\mathrm{ESS},\min} \le SOC_{\mathrm{ESS}} \le SOC_{\mathrm{ESS},\max}, \tag{6}$$

$$P_{\mathrm{Charge}}(t) \le P_{\mathrm{Charge\,max}} {}^{*} X(t), \quad t = 1,2,\ldots T; X \in [0,1], \tag{7}$$

$$P_{\mathrm{Discharge}}(t) \le P_{\mathrm{Discharge\,max}} * Y(t), \quad t = 1,2,\ldots T; X \in [0,1], \tag{8}$$

where $\mathrm{SOC}_{\mathrm{ESS,min}}$ and $\mathrm{SOC}_{\mathrm{ESS,max}}$ are the minimum and maximum state of charge of the storage device. The discharge efficiency is given as

$$\eta_{\mathrm{Discharge}} = \frac{1}{\eta_{\mathrm{Charge}}}. \tag{9}$$

The storage devices cannot charge and discharge at the same time and hence $X(t)$ and $Y(t)$ take values of either 0 or 1. Bus voltage limit for the $i$th bus is given as

$$V_{\min,i} \le V_i \le V_{\max,i}, \quad i \in \{1,2,\ldots N\}, \tag{10}$$

where $V_{\min,i}$ and $V_{\max,i}$ are the minimum and maximum voltage of the $i$th bus.

The current in each feeder should not exceed the maximum current carrying capacity of the branches.

$$|I_K| \le I_{\max}, \quad k \in \{1,2,\ldots l\}, \tag{11}$$

where $l$ is the number of branches. The maximum allowable active and reactive power injection of DGs are as follows.

$$\begin{aligned} P_{\mathrm{DG\,min}} \le P_{\mathrm{DG}} \le P_{\mathrm{DG\,max}}, \\ Q_{\mathrm{DG\,min}} \le Q_{\mathrm{DG}} \le Q_{\mathrm{DG\,max}}, \end{aligned} \tag{12}$$

where $P_{\mathrm{DG}}$ and $Q_{\mathrm{DG}}$ are the active and reactive powers of DGs, $P_{\mathrm{DG\,min}}$ and $Q_{\mathrm{DG\,min}}$ are the minimum allowable active and reactive powers of DGs, and $P_{\mathrm{DG\,max}}$ and $Q_{\mathrm{DG\,max}}$ are the maximum allowable active and reactive powers of DGs.

## 3. Overview of TLBO Algorithm

The Teaching-Learning-Based Optimization (TLBO) algorithm is a new effective human population-based algorithm proposed by Rao et al. This algorithm resembles the teaching-learning process of the instructor and students in a lecture room. In this approach, a set of learners in a category are considered as a population. Also, the number of subjects offered to the learners is the variables, the result of the learner is the fitness value, and the knowledge of the student is the objective function. The parameters considered in the objective function are the variables for the given problem and the best fitness value of the objective function is taken as the best solution. The TLBO method is split into two phases: the teacher phase and the learner phase. In the former phase, the learners are learning from the teacher and in the latter phase, the learners are learning by discussing with other learners [34, 35]. The phases of TLBO are described as follows.

*3.1. Teaching Phase.* In this phase, the teacher continuously tries to improve the mean result of the class for his/her subject. The best solution which is defined by the objective function is considered as the teacher in that population. This phase starts with identifying the best solution. First, generate a random population with $N$ rows and $S$ columns. $N$

represents the population size (number of learners in the class, $i = 1,2, \ldots, N$) and $S$ represents the number of design variables (number of subjects, $j = 1,2, \ldots, S$). The $j$th variable of the $i$th learner is initialized randomly using

$$X_{i,j}^{1} = X_{j}^{\min} + r\text{and} * \left(X_{j}^{\max} - X_{j}^{\min}\right), \tag{13}$$

where rand is a uniformly distributed random number that takes values between 0 and 1 and $X_j^{\min}$ and $X_j^{\max}$ represent the minimum and maximum values for the $j$th parameter. The difference $D_{\text{diff}\,j}^{k}$ between the best solution and the mean result of the class for the $j$th subject in the $k$th iteration is given by

$$D_{\text{diff}\,j}^{k} = r\text{and}\left(X_{T,j}^{k} - T_F M_j^k\right), \tag{14}$$

where $M_j^k$ is the mean result of the students for the subject $j$ and $X_{T,j}^k$ represents the best solution for the subject $j$ in the $k$th iteration. The teaching factor $T_F$ as given in (15) is indicative of the teaching ability of the teacher, depending on which the mean result of the subject will change. Its value is selected as either 1 or 2.

$$T_F = \text{round}[1 + r\text{and}(0,1)]. \tag{15}$$

The solution for the problem is updated in each iteration using

$$X_{\text{new},i,j}^{k} = X_{\text{old},i,j}^{k} + D_{\text{diff}\,j}^{k}, \tag{16}$$

where $X_{\text{new}\,i,j}^{k}$ is the new solution for the $j$th subject and $X_{\text{old}\,i,j}^{k}$ is the old solution for the $j$th subject in the previous iteration. If the updated solution is better than the previous one, it is an acceptable solution. The accepted solution is the input to the next phase.

*3.2. Learner Phase.* This is the second phase of the algorithm in which the learners improve their knowledge through mutual interaction. In this process, each learner will interact with other learners randomly to facilitate knowledge sharing depending on their knowledge level. The solution to the problem is updated based on knowledge sharing. To represent it mathematically, two learners are considered randomly as $X_{(i)}^{k}$ and $X_{(r)}^{k}$. The updated solution can be expressed as follows.

$$X_{\text{new},i}^{k} = \begin{Bmatrix} X_i^k + r\text{and} \times \left(X_i^k - X_r^k\right) & \text{if}\left(X_i^k < X_r^k\right) \\ X_i^k + r\text{and} \times \left(X_r^k - X_i^k\right) & \text{otherwise} \end{Bmatrix}. \tag{17}$$

The best solutions for the different subjects are accepted at the end of this phase, and these solutions are the input for the teacher phase. Both the teacher and learner phases are repeated until the stopping criterion is met. In this work, the stopping criterion is the number of iterations.

*3.3. Implementation of TLBO Algorithm for Energy Management Problem.* In this section, the implementation of the TLBO algorithm for the energy management of generating units and load demand in a VPP is discussed. The steps involved in the implementation procedure are given below.

*Step 1. Initialization of Parameters*

Specify the input data of the VPP and TLBO algorithm. The VPP data includes generator bidding price, hourly utility grid price, load demand, and power limits of the renewable energy sources, storage devices, and distributed generation units. Initialize the parameters of the TLBO algorithm, such as population size, design variables, and stopping criteria. The population size corresponds to the number of students, the number of design variables or subjects offered corresponds to the number of generating units, and the stopping criterion is chosen as the number of iterations.

*Step 2. Initialization of Population*

Generate a random population of dimension $[N \times S]$ according to the population size, $N$, and the number of design variables, $S$. The randomly generated population is mathematically expressed as $X = [X_1, X_2, X_3 \ldots X_N]^T$, where $N$ is the number of solutions in the multidimensional search space. Each solution $X_i = [P_{i1}, P_{i2}, \ldots, P_{ij} \ldots P_{iS}]^T$ is represented by an $S$-dimensional vector, $(i = 1, 2, 3, \ldots N)$ and $(j = 1, 2, 3, \ldots S)$, where $S$ is the number of parameters to be optimized. In this problem, $S$ corresponds to the six DGs. The elements of each solution vector $(X_{ij})$ represent the power output $(P_{gi})$ of distributed generation units that can take values between the maximum and minimum generation limits as given in

$$P_{ij} = P_{j,\min} + \text{rand}(0,1) * \left(P_{j\max} - P_{j\min}\right), \tag{18}$$

where $P_{j\min}$ and $P_{j\max}$ are the minimum and maximum power limits of each unit. For each interval in the scheduling horizon, initialization of the population is done as given in

$$X = \begin{bmatrix} P_{11} & P_{12} & \ldots & P_{1S} \\ P_{21} & P_{22} & \ldots & P_{2S} \\ \vdots & \vdots & \ddots & \vdots \\ P_{N1} & P_{N2} & \ldots & P_{NS} \end{bmatrix}, \tag{19}$$

where $P_{NS}$ is the real power output of the $S$th generation unit for the $N$th individual, which should satisfy the constraint given in (4).

*Step 3. Fitness Evaluation*

Evaluate the generation cost as expressed in (1) for the generated random population in (19) and calculate sum of the cost for all the generating units in the $g^{\text{th}}$ iteration using

$$S^g = \text{Sum}\left(X_{1,j}, X_{2,j}, \ldots X_{i,j}\right). \tag{20}$$

*Step 4. Teacher Phase*

Based on the sum of the generation cost in (20), the minimum generating cost is selected as the best solution. The best solution can be considered as a teacher as expressed in (21). Update the power generation matrix based on the best solution using (16).

$$X_{\text{teacher}} = X \left| f(x) = \min\left(S^g\right)\right|. \tag{21}$$

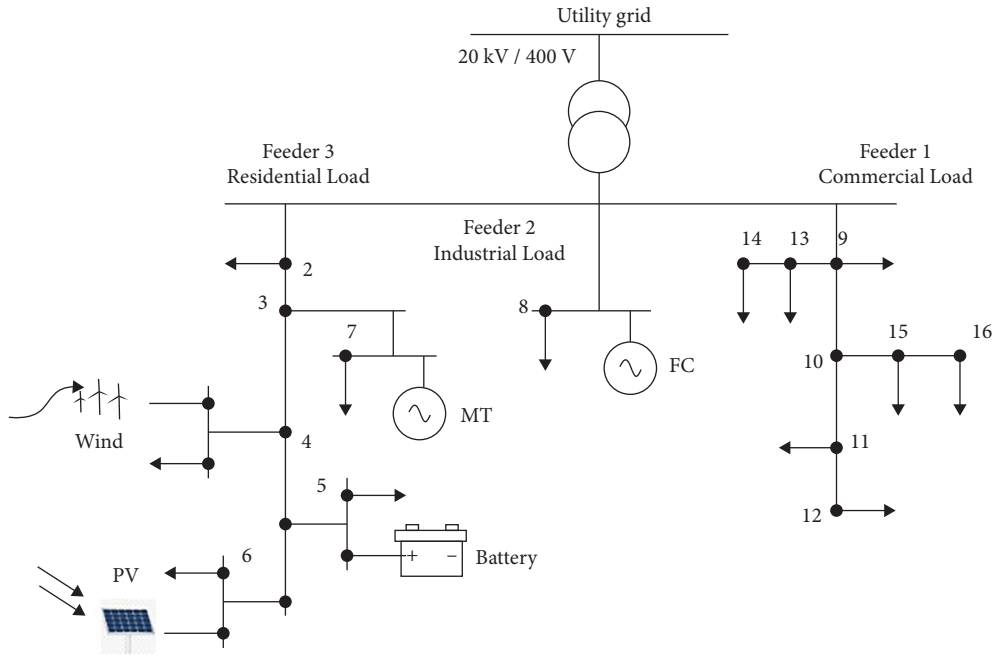


Figure 2: Single-line diagram of IEEE-16-bus test system.

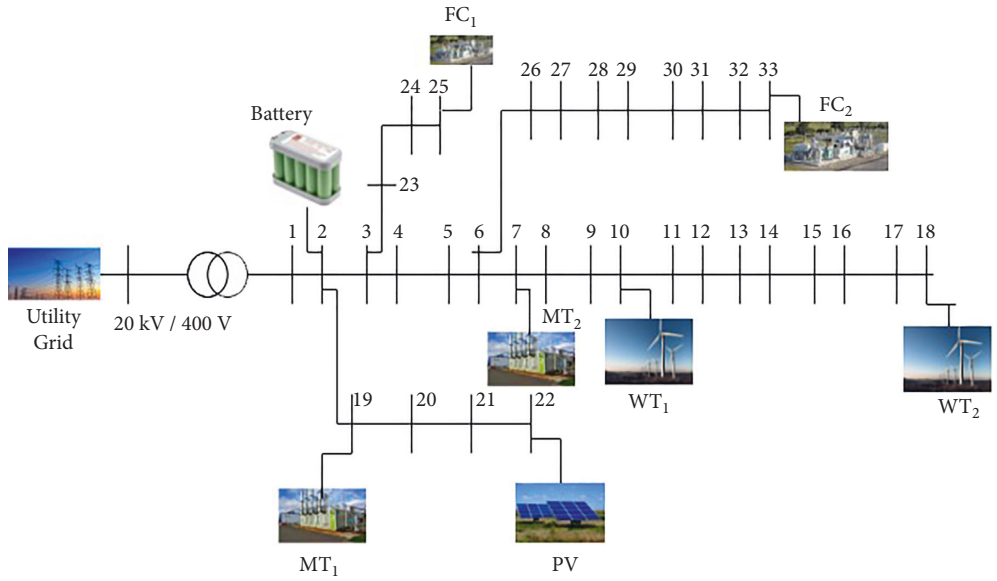


Figure 3: Single-line diagram of IEEE-33-bus test system.

*Step 5. Learner Phase*

In this step, the best solution obtained in Step 4 is considered as the input for the learner phase. The solution is modified based on the mutual interaction among the learners and the solution matrix is updated using (17).

*Step 6.* Repeat steps 3–5 until the stopping criterion is met, which is the maximum number of iterations.

## 4. Results and Discussions

In this section, the cost minimization problem of a VPP is implemented using the TLBO algorithm. IEEE-16[32, 36] and IEEE-33 [37] bus test systems shown in Figures 2 and 3 are considered in this paper. They comprise of wind, solar, microturbine, and fuel cell as generating units, along with the storage devices and loads. The optimal load dispatch is done for 24 hours in a day, and the optimal power generation is based on the utility price and the load demand at the particular hour. Programming is done in MATLAB for the aforementioned problem and executed on Intel® Core™ i7-8550U, 8th Gen CPU @ 1.99 GHz, 8.00 GB RAM PC. The power limits, bidding price, and start-up/shutdown cost of each generating unit for IEEE 16-bus and IEEE 33-bus test systems are given in Tables 1 and 2, respectively. The load demand, utility market price, and forecasted power output

Table 1: Input data of IEEE-16-bus system.

| ID | Type | Minimum power (kW) | Maximum power (kW) | Bid (€ct/kWh) | Start-up/shutdown cost (€ct) |
|---|---|---|---|---|---|
| 1 | MT | 6 | 30 | 0.457 | 0.96 |
| 2 | FC | 3 | 30 | 0.294 | 1.65 |
| 3 | PV | 0 | 25 | 2.584 | 0 |
| 4 | WT1 | 0 | 15 | 1.073 | 0 |
| 5 | Battery | −30 | 30 | 0.38 | 0 |
| 6 | Utility | −30 | 30 | — | 0 |

Table 2: Input data of IEEE-33-bus system.

| ID | Type | Minimum power (kW) | Maximum power (kW) | Bid (€ct/kWh) | Start-up/shutdown cost (€ct) |
|---|---|---|---|---|---|
| 1 | MT1 | 6 | 30 | 0.457 | 0.96 |
| 2 | FC1 | 3 | 30 | 0.294 | 1.65 |
| 3 | PV | 0 | 25 | 2.584 | 0 |
| 4 | WT1 | 0 | 15 | 1.073 | 0 |
| 5 | Battery | −30 | 30 | 0.38 | 0 |
| 6 | Utility | −30 | 30 | — | 0 |
| 7 | WT2 | 0 | 35 | 1.969 | 0 |
| 8 | MT2 | 8 | 50 | 0.269 | 0.96 |
| 9 | FC2 | 8 | 50 | 0.275 | 1.65 |

Table 3: Total load demand of IEEE-16-bus and IEEE-33-bus test systems.

| Hr | IEEE-16-bus load demand (kW) | IEEE-33-bus load demand (kW) |
|---|---|---|
| 1 | 52 | 133.75 |
| 2 | 50 | 114.75 |
| 3 | 50 | 114.75 |
| 4 | 51 | 138.25 |
| 5 | 56 | 140.50 |
| 6 | 63 | 125.25 |
| 7 | 70 | 128.75 |
| 8 | 75 | 132.75 |
| 9 | 76 | 138.25 |
| 10 | 80 | 148.50 |
| 11 | 78 | 162.75 |
| 12 | 74 | 170.25 |
| 13 | 72 | 178.50 |
| 14 | 72 | 160.50 |
| 15 | 76 | 155.25 |
| 16 | 80 | 145.75 |
| 17 | 85 | 140.25 |
| 18 | 88 | 98.75 |
| 19 | 90 | 102.25 |
| 20 | 87 | 135.50 |
| 21 | 78 | 120.25 |
| 22 | 71 | 133.75 |
| 23 | 65 | 145.50 |
| 24 | 56 | 130.25 |

Table 4: Utility price for IEEE 16-bus and IEEE 33-bus test systems.

| Hr | Utility price (€ct/kWh) |
|---|---|
| 1 | 0.23 |
| 2 | 0.19 |
| 3 | 0.14 |
| 4 | 0.12 |
| 5 | 0.12 |
| 6 | 0.20 |
| 7 | 0.23 |
| 8 | 0.38 |
| 9 | 1.50 |
| 10 | 4.00 |
| 11 | 4.00 |
| 12 | 4.00 |
| 13 | 1.50 |
| 14 | 4.00 |
| 15 | 2.00 |
| 16 | 1.95 |
| 17 | 0.60 |
| 18 | 0.41 |
| 19 | 0.35 |
| 20 | 0.43 |
| 21 | 1.17 |
| 22 | 0.54 |
| 23 | 0.30 |
| 24 | 0.26 |

[32] from PV, Wind1, and Wind2 are given in Tables 3–5, respectively. The total load demand per day is taken as 1695 kW and 3295 kW for IEEE 16-bus and IEEE 33-bus test systems, respectively. The power losses are computed using the forward-backward sweep method [33]. The base power and base voltage are taken as 100 kVA and 400 V, respectively, and the cost for the power losses is assumed as 0.19 (€ct/kWh). The power factor is taken as 0.85 lagging for residential and commercial loads and 0.9 lagging for industrial loads [38] for both IEEE 16- and IEEE 33-bus test systems. The optimization problem is solved for with and without losses for comparison purpose. In addition to the TLBO algorithm, ABC and ALO algorithms are also used in this paper to solve the problem statement and to validate the performance of the TLBO algorithm.

The parameters of the TLBO algorithm used in this problem are the population size, $N$ taken as 100, maximum iteration as 1000, and number of trials or runs as 20. The

Table 5: Forecasted output of PV, WT1, and WT2.

| Hr | PV (kW) | WT1 (kW) | WT2 (kW) |
|---|---|---|---|
| 1 | 0 | 1.7850 | 4.165 |
| 2 | 0 | 1.7850 | 4.165 |
| 3 | 0 | 1.7850 | 4.165 |
| 4 | 0 | 1.7850 | 4.165 |
| 5 | 0 | 1.7850 | 4.165 |
| 6 | 0 | 0.9142 | 2.135 |
| 7 | 0 | 1.7850 | 4.165 |
| 8 | 0.1937 | 1.3017 | 3.045 |
| 9 | 3.7540 | 1.7850 | 4.165 |
| 10 | 7.5290 | 3.0854 | 7.210 |
| 11 | 10.4410 | 8.7724 | 20.475 |
| 12 | 11.9640 | 10.413 | 24.290 |
| 13 | 23.8930 | 3.9228 | 9.135 |
| 14 | 21.0490 | 2.3766 | 5.53 |
| 15 | 7.8647 | 1.7850 | 4.165 |
| 16 | 4.2208 | 1.3017 | 3.045 |
| 17 | 0.5389 | 1.7850 | 4.165 |
| 18 | 0 | 1.7850 | 4.165 |
| 19 | 0 | 1.3017 | 3.038 |
| 20 | 0 | 1.7850 | 4.165 |
| 21 | 0 | 1.3017 | 3.0345 |
| 22 | 0 | 1.3017 | 3.0345 |
| 23 | 0 | 0.9142 | 2.135 |
| 24 | 0 | 0.6124 | 1.435 |

Table 6: Optimal power dispatch using TLBO Case I.

| Hr | MT (kW) | FC (kW) | PV (kW) | WT1 (kW) | Battery (kW) | Utility (kW) | SOC (kW) |
|---|---|---|---|---|---|---|---|
| 1 | 6.000 | 16.563 | 0 | 1.7850 | −2.348 | 30.0000 | 5.348 |
| 2 | 6.000 | 15.057 | 0 | 1.7850 | −2.842 | 30.0000 | 8.190 |
| 3 | 6.000 | 15.654 | 0 | 1.7850 | −3.439 | 30.0000 | 11.629 |
| 4 | 6.000 | 17.038 | 0 | 1.7850 | −3.823 | 30.0000 | 15.452 |
| 5 | 6.000 | 22.342 | 0 | 1.7850 | −4.127 | 30.0000 | 19.579 |
| 6 | 6.000 | 29.061 | 0 | 0.9142 | −2.975 | 30.0000 | 22.554 |
| 7 | 10.709 | 30 | 0 | 1.7850 | −2.494 | 30.0000 | 25.048 |
| 8 | 15.457 | 30 | 0.1937 | 1.3017 | −1.952 | 30.0000 | 27.000 |
| 9 | 30.000 | 30 | 3.7540 | 1.7850 | 1.792 | 8.669 | 25.208 |
| 10 | 30.000 | 30 | 7.5290 | 3.0854 | 2.698 | 6.689 | 22.510 |
| 11 | 30.000 | 30 | 10.4410 | 8.7724 | 3.325 | −4.538 | 19.185 |
| 12 | 30.000 | 30 | 11.9640 | 10.413 | 3.519 | −11.896 | 15.666 |
| 13 | 30.000 | 30 | 23.8930 | 3.9228 | 1.414 | −17.230 | 14.252 |
| 14 | 30.000 | 30 | 21.0490 | 2.3766 | 3.689 | −15.115 | 10.563 |
| 15 | 30.000 | 30 | 7.8647 | 1.7850 | 2.384 | 3.966 | 8.179 |
| 16 | 30.000 | 30 | 4.2208 | 1.3017 | 1.548 | 12.930 | 6.631 |
| 17 | 30.000 | 30 | 0.5389 | 1.7850 | 1.468 | 21.208 | 5.163 |
| 18 | 24.828 | 30 | 0 | 1.7850 | 1.387 | 30.000 | 3.776 |
| 19 | 30.000 | 30 | 0 | 1.3017 | −1.302 | 30.000 | 5.078 |
| 20 | 24.569 | 30 | 0 | 1.7850 | 0.646 | 30.000 | 4.432 |
| 21 | 30.000 | 30 | 0 | 1.3017 | 0.928 | 15.770 | 3.504 |
| 22 | 30.000 | 30 | 0 | 1.3017 | 0.501 | 9.197 | 3.003 |
| 23 | 6.000 | 30 | 0 | 0.9142 | −1.154 | 29.240 | 4.157 |
| 24 | 6.000 | 20.715 | 0 | 0.6124 | −1.327 | 30.0000 | 5.484 |

same parameters are used for ABC and ALO algorithms for comparison. Four different cases are considered, and the results are discussed in this section.

Power is exchanged between the VPP and the grid, based on the bidding price of the generation units and that of the utility grid. Whenever the bidding price of the DGs in the VPP is less than that of the utility price, the generated VPP power is used to meet the load demand. Also, the excess power generated and the energy stored in the storage devices (discharging mode) are sold to the utility grid. If the bidding

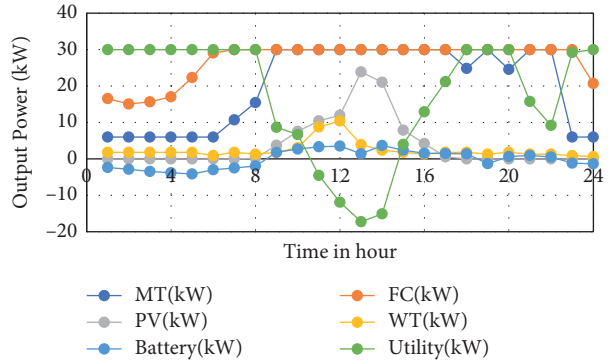


Figure 4: Optimal schedule of DGs and the utility–Case I.

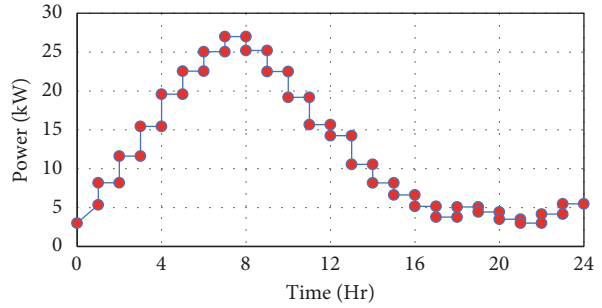


Figure 5: State of charge of battery–Case I.

Table 7: Comparison of the total cost—Case I.

| Method | Best solution (€ct) | Worst solution (€ct) | Mean (€ct) | Simulation time (s) |
|---|---|---|---|---|
| Without losses | | | | |
| ABC | 768.9008 | 773.4415 | 769.0444 | 7.998 |
| ALO | 767.6991 | 772.4553 | 767.8516 | 7.584 |
| TLBO | 765.2968 | 771.6939 | 765.4500 | 6.341 |
| With losses | | | | |
| ABC | 761.9520 | 766.4927 | 762.0956 | 8.214 |
| ALO | 760.7503 | 765.5065 | 760.9028 | 7.982 |
| TLBO | 758.3480 | 764.7451 | 758.5042 | 6.587 |

price of the VPP is greater than that of the utility price, the power is bought from the utility grid and the same is stored in the storage devices (charging mode). In general, the power generated by the PV and wind is utilized based on their maximum availability. FC and MT are operated throughout the day because of lower bid costs.

*4.1. Case I.* In this case, all the generating units in the VPP are in operation and they operate within their power limits. The VPP is connected to the utility grid. The maximum power which can be exchanged between the VPP and the utility grid is restricted to 30 kW. All the DGs except PV are in ON condition throughout the 24 hours. The initial SOC of the storage device is taken as 3 kW (i.e., 10% of the maximum capacity). The optimal power dispatch for 24 hours of the day using the TLBO algorithm is given in Table 6. Each

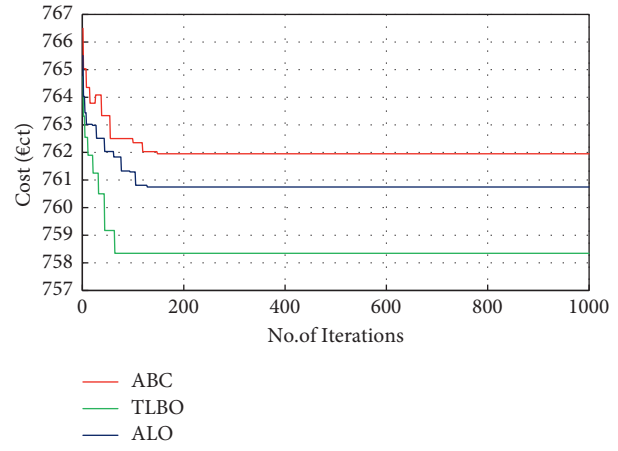


Figure 6: Comparison of convergence characteristics for Case I.

Table 8: Optimal power dispatch using TLBO algorithm—Case II.

| Hr | MT (kW) | FC (kW) | PV (kW) | WT1 (kW) | Battery (kW) | Utility (kW) | SOC (kW) |
|---|---|---|---|---|---|---|---|
| 1 | 6.000 | 3 | 0 | 1.7850 | −2.213 | 43.428 | 5.213 |
| 2 | 6.000 | 3 | 0 | 1.7850 | −2.742 | 41.957 | 7.955 |
| 3 | 6.000 | 3 | 0 | 1.7850 | −3.514 | 42.729 | 11.469 |
| 4 | 6.000 | 3 | 0 | 1.7850 | −3.867 | 44.082 | 15.336 |
| 5 | 6.000 | 3 | 0 | 1.7850 | −4.315 | 49.53 | 19.651 |
| 6 | 6.000 | 3 | 0 | 0.9142 | −2.813 | 55.899 | 22.464 |
| 7 | 6.000 | 3 | 0 | 1.7850 | −2.584 | 61.799 | 25.048 |
| 8 | 6.000 | 30 | 0.1937 | 1.3017 | −1.952 | 39.456 | 27.000 |
| 9 | 30.000 | 30 | 3.7540 | 1.7850 | 1.592 | 8.869 | 25.408 |
| 10 | 29.999 | 30 | 7.5290 | 3.0854 | 2.986 | 6.4007 | 22.422 |
| 11 | 29.999 | 30 | 10.4410 | 8.7724 | 3.821 | −5.0344 | 18.601 |
| 12 | 29.990 | 30 | 11.9640 | 10.413 | 3.519 | −11.8963 | 15.082 |
| 13 | 29.999 | 30 | 23.8930 | 3.9228 | 1.214 | −17.0298 | 13.868 |
| 14 | 29.992 | 30 | 21.0490 | 2.3766 | 3.689 | −15.1146 | 10.179 |
| 15 | 30.000 | 30 | 7.8647 | 1.7850 | 2.464 | 3.8863 | 7.715 |
| 16 | 29.999 | 30 | 4.2208 | 1.3017 | 1.548 | 12.9295 | 6.167 |
| 17 | 30.000 | 30 | 0.5389 | 1.7850 | 1.068 | 21.6081 | 5.099 |
| 18 | 25.128 | 30 | 0 | 1.7850 | 1.397 | 48.818 | 3.702 |
| 19 | 30.000 | 30 | 0 | 1.3017 | −1.3017 | 54 | 5.004 |
| 20 | 26.538 | 30 | 0 | 1.7850 | 0.646 | 48.569 | 4.358 |
| 21 | 30.000 | 30 | 0 | 1.3017 | 0.839 | 15.8593 | 3.519 |
| 22 | 29.998 | 30 | 0 | 1.3017 | 0.519 | 9.1793 | 3.000 |
| 23 | 6.000 | 30 | 0 | 0.9142 | −1.124 | 29.2098 | 4.124 |
| 24 | 6.000 | 3 | 0 | 0.6124 | −1.243 | 47.6306 | 5.367 |

unit is optimally operated based on its bidding price and the load demand.

During the first eight hours of the day, the bid cost of the utility is lesser than that of any of the DGs (except FC) in the VPP. Thereby, 30 kW of power is purchased from the utility grid and the remaining load demand is supplied by the DGs in the VPP as shown in Figure 4. For instance, at the 8th hour, the demand is 75 kW. So, 30 kW is purchased from the utility and the remaining 45 kW is supplied by the DGs in the VPP. As FC has the lowest bid cost, it supplies its maximum capacity of 30 kW, and the remaining 10 kW is supplied by PV, wind, MT, and battery.

Also, the load demand is less during the first eight hours and thereby, the excess power generated in the VPP is stored in the battery. The SOC of the battery is plotted in Figure 5. At the end of the 8th hour, the battery is charged to 90% of its maximum capacity (27 kW).

After the 8th hour, it can be observed that the utility grid price is higher than that of the other DGs (except PV) in the VPP. The demand is also higher. Now, the local demand in the VPP is met by the DGs and the excess power generated is exported to the utility. The battery is in discharging mode to meet the excess load demand. It is also observed from Figure 5 that at the end of the 18th hour of the day, the battery is discharged to 10% of its maximum capacity (3.776 kW).

For instance, at the 18th hour, the load demand is 88 kW. The available wind power is 1.7085 kW, battery power of 1.387 kW, and microturbine power of 24.828 kW are used to meet the demand along with the utility power and fuel cell power of 30 kW each. There is no PV power availability from the 18th hour. During these hours, the load demand in the

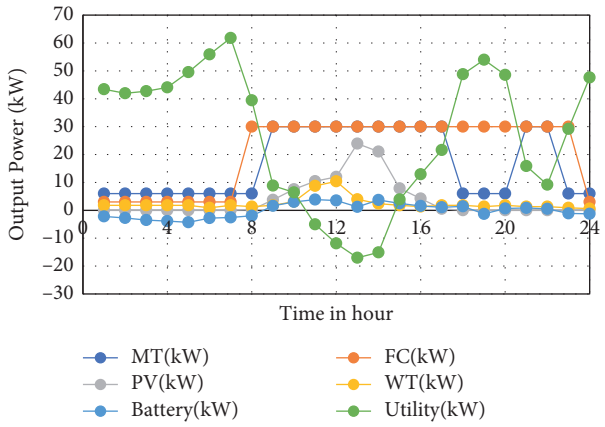


Figure 7: Optimal schedule of DGs and the utility—Case II.

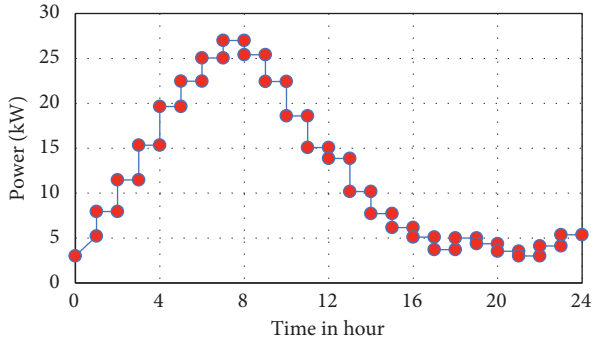


Figure 8: State of charge of the battery—Case II.

Table 9: Comparison of the total cost—Case II.

| Method | Best solution (€ct) | Worst solution (€ct) | Mean (€ct) | Simulation time (s) |
|---|---|---|---|---|
| Without losses | | | | |
| ABC | 748.8728 | 755.2788 | 749.1978 | 7.982 |
| ALO | 745.6808 | 756.0728 | 746.2068 | 7.245 |
| TLBO | 742.5108 | 753.2698 | 742.7778 | 6.153 |
| With losses | | | | |
| ABC | 741.924 | 748.330 | 742.249 | 8.124 |
| ALO | 738.732 | 749.124 | 739.258 | 7.845 |
| TLBO | 735.562 | 746.321 | 735.829 | 6.524 |

VPP is met with the other sources based on their bidding price. During the last two hours of the day, the power demand is less and the excess power is stored in the battery. At the end of the day, the SOC of the battery for Case I is 5.484 kW. The operating cost of VPP (with losses) for the Case I is obtained using the TLBO method and is compared with other metaheuristic techniques and is given in Table 7. It is evident from the results that TLBO is superior to other methods as it provides the minimum cost of €ct 758.348 for without losses and €ct 765.2968 for with losses. The comparison of convergence characteristics for the optimal operating cost for Case I is illustrated in Figure 6. It is observed that the optimal solution is obtained within 100 iterations when compared to the ABC and ALO methods. From Table 7, it can be observed that the time taken for the convergence of optimal solution using the TLBO algorithm is 6.587 s, which is lesser than that of the other methods.

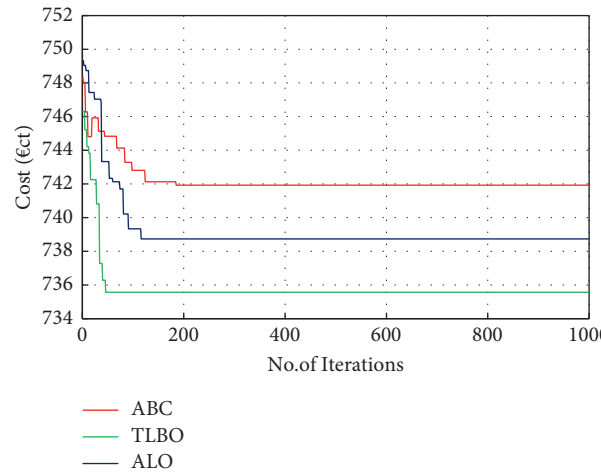


Figure 9: Comparison of convergence characteristics—Case II.

*4.2. Case II.* In this case, the DGs operate within their power limits and there is no restriction on the power exchange between the utility grid and the VPP. All the DGs are in ON condition throughout the 24-hour time period except for PV. The initial SOC of the storage device is 3 kW, which is 10% of the maximum battery capacity. The optimal power dispatch for 24 hours of the day using the TLBO algorithm is shown in Table 8. In Figure 7, it is observed that for the first 7 hours of the day, the utility grid price is low compared with the bidding price of the DGs in the VPP. Hence, energy is purchased from the utility grid without any restriction to meet the load demand of VPP. The power output from the PV and wind turbine are used as per the availability. All other units of VPP are operating with minimum capacity due to their higher bidding price compared to the utility price.

During the first 8 hours, the load demand is less. Therefore, the excess power is stored in the battery. At the end of the 8th hour, the battery is charged to 90% of its maximum capacity (27 kW) and is shown in Figure 8. The load demand increases from the 9th hour of the day. The utility price is higher than that of the VPP bidding price from the 9th to the 18th hour of the day. Thereby, power is sold to the utility grid without any restrictions. The battery is in discharging mode to meet the load demand. The SOC of the battery will change depending on the load demand and the bid cost. The battery is discharged to 3.702 kW (10% of its maximum capacity). During the 9th to 18th hour of the day, the available power generation from the wind is utilized to meet the load demand. Since the utility price is more than the bidding price of MT and FC, these units are operating with their maximum capacity to meet the load demand. From the 18th to the 20th hours of the day, the load demand is high (peak load). During this period, PV power is not available and also wind power availability is less. As the bid cost of fuel cell power is less, it is operated at its maximum capacity. In addition, the utility power price is also less and thereby power is purchased from the utility. Power is also stored in the storage devices during this interval.

The discussions made for the 18th to 20th hours are valid for the 23rd and 24th hours also. During the 20th and 22nd hours of the day, as the utility price is more than that of VPP, power is sold from the VPP to the utility grid. All the units are operating with maximum capacity and the battery is also supplying the power. On the 22nd hour, the battery has discharged to 3 kW (10% of its maximum capacity) as shown in Figure 8. During the last two hours of the day, the power demand is less and the excess power is stored in the battery. At the end of the day, the SOC of the battery for Case II is 5.367 kW.

The operating cost (with losses) for Case II using the TLBO algorithm is shown in Table 9 and is compared with the other metaheuristic techniques like ABC and ALO. From Table 9, it is noticed that TLBO is better than other techniques in terms of convergence time and operating cost. The convergence graph for Case II is shown in Figure 9. It is

Table 10: Optimal power dispatch using TLBO algorithm—Case III.

| Hr | Unit On/Off status | MT (kW) | FC (kW) | PV (kW) | WT1 (kW) | Battery (kW) | Utility (kW) | SOC (kW) |
|---|---|---|---|---|---|---|---|---|
| 1 | 010111 | 0 | 29.383 | 0 | 1.7850 | −2.481 | 23.313 | 5.481 |
| 2 | 010111 | 0 | 26.241 | 0 | 1.7850 | −3.042 | 25.016 | 8.523 |
| 3 | 110111 | 6.001 | 15.340 | 0 | 1.7850 | −3.125 | 30.000 | 11.648 |
| 4 | 110111 | 6.003 | 17.232 | 0 | 1.7850 | −4.018 | 29.999 | 15.666 |
| 5 | 010111 | 0 | 29.209 | 0 | 1.7850 | −4.127 | 29.132 | 19.793 |
| 6 | 110111 | 6.000 | 28.999 | 0 | 0.9142 | −2.912 | 29.999 | 22.705 |
| 7 | 110111 | 10.459 | 30 | 0 | 1.7850 | −2.243 | 29.999 | 24.948 |
| 8 | 111111 | 15.557 | 30 | 0.194 | 1.3017 | −2.052 | 30.000 | 27.000 |
| 9 | 111111 | 30.000 | 29.998 | 3.754 | 1.7850 | 1.568 | 8.895 | 25.432 |
| 10 | 111111 | 29.991 | 29.998 | 7.529 | 3.0854 | 2.995 | 6.403 | 22.437 |
| 11 | 111111 | 30.000 | 29.974 | 10.441 | 8.7724 | 3.448 | −4.636 | 18.989 |
| 12 | 111111 | 29.999 | 29.997 | 11.964 | 10.413 | 4.212 | −12.585 | 14.777 |
| 13 | 111111 | 29.962 | 29.999 | 23.893 | 3.9228 | 1.617 | −17.393 | 13.160 |
| 14 | 111111 | 29.999 | 29.988 | 21.049 | 2.3766 | 3.571 | −14.984 | 9.589 |
| 15 | 111111 | 29.996 | 29.999 | 7.8647 | 1.7850 | 2.786 | 3.609 | 6.803 |
| 16 | 111111 | 30.000 | 30 | 4.2208 | 1.3017 | 1.353 | 13.125 | 5.450 |
| 17 | 111111 | 30.000 | 30 | 0.5389 | 1.7850 | 1.363 | 21.313 | 4.087 |
| 18 | 110111 | 25.128 | 30 | 0 | 1.7850 | 1.087 | 30.000 | 3.000 |
| 19 | 110111 | 30.000 | 30 | 0 | 1.3017 | −1.302 | 30.000 | 4.302 |
| 20 | 110111 | 26.414 | 30 | 0 | 1.7850 | −1.198 | 30.000 | 5.500 |
| 21 | 110111 | 30.000 | 30 | 0 | 1.3017 | 1.288 | 15.411 | 4.212 |
| 22 | 110111 | 30.000 | 30.000 | 0 | 1.3017 | 1.211 | 8.488 | 3.001 |
| 23 | 110111 | 6.000 | 29.997 | 0 | 0.9142 | −1.254 | 29.343 | 4.255 |
| 24 | 010111 | 0 | 29.448 | 0 | 0.6124 | −1.927 | 27.868 | 6.182 |

evident from the characteristics that TLBO is faster than the other two methods. The convergence time for this problem using TLBO is 6.524 s.

*4.3. Case III.* In this case, all the generating units in the VPP can switch between the ON/OFF modes and they operate within their power limits. The initial SOC of the storage device is 3 kW. The VPP is connected to the utility grid. The maximum power that can be exchanged between the VPP and the utility grid is restricted to 30 kW.

The optimal power dispatch for 24 hours of the day using the TLBO algorithm is presented in Table 10. The ON and OFF states of the MT, FC, PV, WT1, battery, and utility are represented by 1 and 0, respectively. From Figure 10, it is evident that, for the first 8 hours of the day, the utility grid price is low compared with the VPP bidding price. Hence, power is purchased from the utility grid to meet the load demand of VPP and the storage device is in charging mode.

At the end of the 8th hour, the battery is charged to 90% of the maximum capacity; that is, the SOC is 27 kW as depicted in Figure 11. During this period, the power output from the PV is zero. The bidding price of FC is less compared to all the other units of VPP. Hence, FC is operating at its maximum capacity during this period.

The utility price is higher than that of the VPP bidding price from the 9th to 18th hours of the day. Thereby, the power is sold to the utility grid by discharging the storage devices. The battery is in discharging mode and discharged to 10% of its maximum capacity (i.e., 3.5 kW during the 18th hour as shown in the SOC plot in Figure 11). During this duration, the power generation from the RES (PV and wind) are utilized as per the availability.

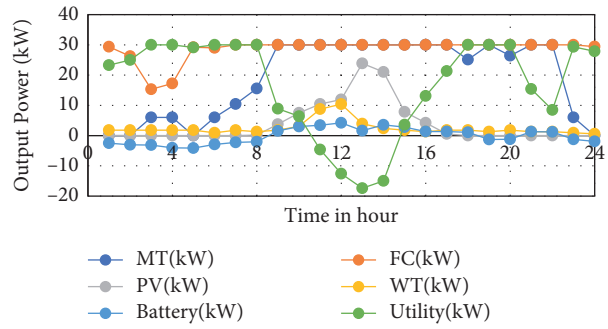


Figure 10: Optimal schedule of DGs and the utility—Case III.

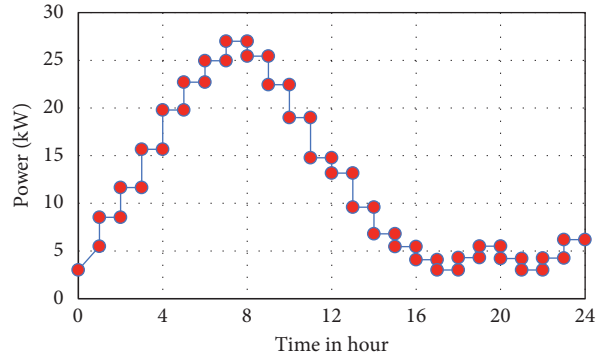


Figure 11: State of charge of the battery—Case III.

From the 19th and 20th hours of the day, the load demand is high (peak load). During this period, the bidding price of FC is less and is operating with its maximum capacity. Since the utility price is less compared to the VPP

Table 11: Comparison of the total cost—Case III.

| Method | Best solution (€ct) | Worst solution (€ct) | Mean (€ct) | Simulation time (s) |
|---|---|---|---|---|
| Without losses | | | | |
| ABC | 766.4057 | 780.2791 | 767.0253 | 7.840 |
| ALO | 761.3383 | 779.1642 | 762.0748 | 7.568 |
| TLBO | 758.6558 | 777.9809 | 759.1309 | 6.548 |
| With losses | | | | |
| ABC | 759.4569 | 773.3303 | 760.0765 | 8.012 |
| ALO | 754.3895 | 772.2154 | 755.1260 | 7.812 |
| TLBO | 751.707 | 771.0321 | 752.1821 | 6.987 |

bidding price, the grid power along with the power generated from the VPP is used to meet the peak load. Also, the storage device is in discharging mode. During the 21st and 22nd hours of the day, as the utility price is more than that of VPP, the power from VPP is sold to the utility grid. Since the bidding price of FC and MT is less compared with that of the utility price, these units are operating at their maximum capacity. The battery is in discharging mode and discharged to 10% of maximum capacity (i.e., 3.122 kW during the 18th hour as shown in the SOC plot in Figure 11). During the 23rd and 24th hours of the day, the utility price is less than that of VPP, so power is purchased from the utility to VPP and stored in the storage devices (charging mode). During the last two hours of the day, the power demand is less and the excess power is stored in the battery. The operating cost (with losses) using the TLBO algorithm for Case III is compared with the other metaheuristic techniques and is given in Table 11. Minimum operating cost is obtained using the TLBO algorithm when compared with other methods. The convergence characteristics with respect to the number of iterations is plotted in Figure 12. It is observed that the optimal solution is obtained in minimum time and less number of iterations using the TLBO algorithm. The time taken for the convergence using the TLBO algorithm is 6.987 s.

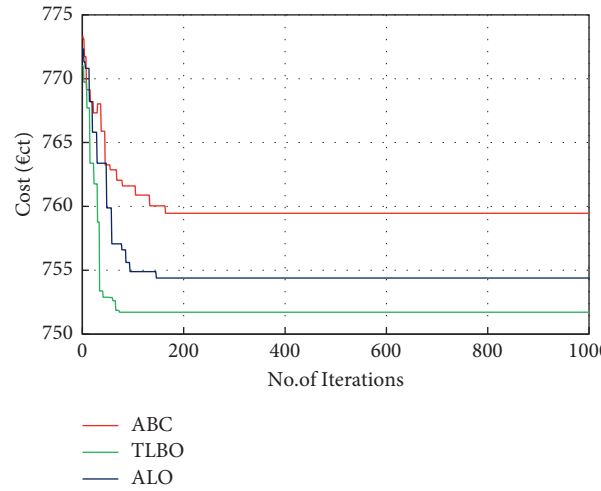


Figure 12: Comparison of convergence characteristics—Case III.

*4.4. Case IV.* In this case, the IEEE-33 bus test system is considered. All the generating units of VPP are in ON condition and operating within their respective power limits. The maximum amount of power that can be transferred between the VPP and the utility grid is considered as 30 kW. Throughout the day, all DGs are available to meet the load demand, except PV. The initial SOC of the battery is assumed to be 3 kW, which is 10% of its maximum capacity. The optimal power dispatch for 24 hours of the day using the TLBO algorithm is shown in Table 12. Each unit is operated within its capacity based on its bidding price and load demand. Furthermore, power is transferred between the VPP and the utility grid based on the bidding price.

From Figure 13, it can be observed that, during the first seven hours of the day, the bid cost of the utility is lesser than that of any of the DGs in VPP. As a result, 30 kW of power is bought from the utility grid and the remaining load demand is supplied by the DGs in the VPP based on their bid cost. For instance, at the 7th hour, the demand is 128.75 kW. Therefore 30 kW of power is purchased from the utility, while the remaining 98.75 kW is supplied by the VPP units. As MT2 has the lowest bid cost, it supplies its maximum capacity of 50 kW and the remaining 48.75 kW is supplied by other units. During the first 8 hours, the load demand is less. Therefore, the excess power is stored in the battery. The SOC of the battery is plotted in Figure 14. At the end of the 8th hour, the SOC of the battery is 90% of its maximum capacity (27.03 kW) as displayed in Figure 14.

In general, the power generated by PV and wind is utilized based on their maximum availability. MT2 is operated with its maximum capacity throughout the day because of the lower bid cost. After the 7th hour, it can be observed that the utility grid price is more compared to the other DG units in the VPP. The demand is also higher. Now, the local demand in the VPP is met by the DGs and the excess power generated is exported to the utility. From the 8th to 22nd hours of the day, FC1, MT2, and FC2 have lesser bid cost compared to the utility grid. Hence, these units are operating at their maximum capacity during this period. The battery is in discharging mode to meet the excess load demand. It is also observed from Figure 14 that at the end of the 22nd hour of the day, the battery is discharged to 10% of its maximum capacity (3.071 kW). For instance, at the 22nd hour, the load demand is 133.75 kW. To meet this demand, 4.337 kW total available power from the RES, battery power

Table 12: Optimal power dispatch using TLBO algorithm—Case IV.

| Hr | MT1 (kW) | FC1 (kW) | PV (kW) | WT1 (kW) | WT2 (kW) | MT2 (kW) | FC2 (kW) | Bat (kW) | Utility (kW) | SOC (kW) |
|---|---|---|---|---|---|---|---|---|---|---|
| 1 | 6 | 3 | 0 | 1.785 | 4.165 | 50 | 40.998 | −2.198 | 30 | 5.198 |
| 2 | 6 | 3 | 0 | 1.785 | 4.165 | 50 | 22.767 | −2.967 | 30 | 8.165 |
| 3 | 6 | 3 | 0 | 1.785 | 4.165 | 50 | 23.050 | −3.250 | 30 | 11.415 |
| 4 | 6 | 3 | 0 | 1.785 | 4.165 | 50 | 47.123 | −3.823 | 30 | 15.238 |
| 5 | 6 | 3.302 | 0 | 1.785 | 4.165 | 50 | 50.000 | −4.752 | 30 | 19.99 |
| 6 | 6 | 3 | 0 | 0.914 | 2.135 | 50 | 35.946 | −2.745 | 30 | 22.735 |
| 7 | 6 | 3 | 0 | 1.785 | 4.165 | 50 | 35.943 | −2.143 | 30 | 24.878 |
| 8 | 6 | 30 | 0.194 | 1.302 | 3.045 | 50 | 50 | −2.152 | −5.638 | 27.03 |
| 9 | 26.888 | 30 | 3.754 | 1.785 | 4.165 | 50 | 50 | 1.658 | −30 | 25.372 |
| 10 | 27.831 | 30 | 7.528 | 3.085 | 7.210 | 50 | 50 | 2.846 | −30 | 22.526 |
| 11 | 19.794 | 30 | 10.441 | 8.772 | 20.475 | 50 | 50 | 3.268 | −30 | 19.258 |
| 12 | 19.602 | 30 | 11.964 | 10.413 | 24.290 | 50 | 50 | 3.981 | −30 | 15.277 |
| 13 | 30 | 30 | 23.893 | 3.923 | 9.135 | 50 | 50 | 1.864 | −20.315 | 13.413 |
| 14 | 28.087 | 30 | 21.049 | 2.377 | 5.530 | 50 | 50 | 3.457 | −30 | 9.956 |
| 15 | 30 | 30 | 7.865 | 1.785 | 4.165 | 50 | 50 | 2.876 | −21.441 | 7.08 |
| 16 | 30 | 30 | 4.221 | 1.302 | 3.045 | 50 | 50 | 1.765 | −24.583 | 5.315 |
| 17 | 30 | 30 | 0.539 | 1.785 | 4.165 | 50 | 50 | 1.212 | −27.451 | 4.103 |
| 18 | 6 | 15.813 | 0 | 1.785 | 4.165 | 50 | 50 | 0.987 | −30 | 3.116 |
| 19 | 6 | 24.755 | 0 | 1.302 | 3.038 | 50 | 50 | −2.845 | −30 | 5.961 |
| 20 | 6 | 30 | 0 | 1.785 | 4.165 | 50 | 50 | 0.885 | −7.335 | 5.076 |
| 21 | 14.893 | 30 | 0 | 1.302 | 3.035 | 50 | 50 | 1.021 | −30 | 4.055 |
| 22 | 28.430 | 30 | 0 | 1.302 | 3.035 | 50 | 50 | 0.984 | −30 | 3.071 |
| 23 | 6 | 30 | 0 | 0.914 | 2.135 | 50 | 50 | −1.216 | 7.667 | 4.287 |
| 24 | 6 | 3 | 0 | 0.612 | 1.435 | 50 | 40.715 | −1.512 | 30 | 5.799 |

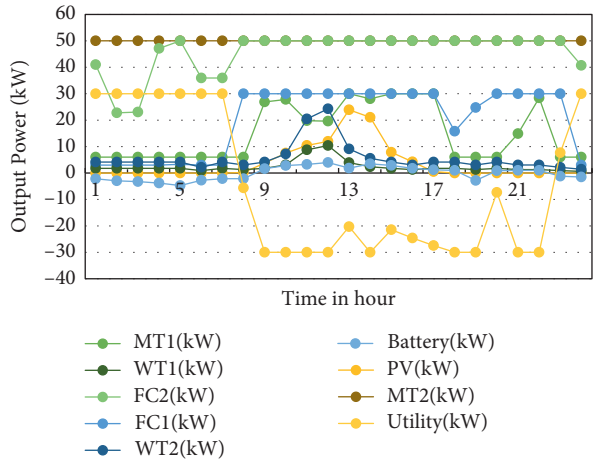


Figure 13: Optimal schedule of DGs and the utility—Case IV.

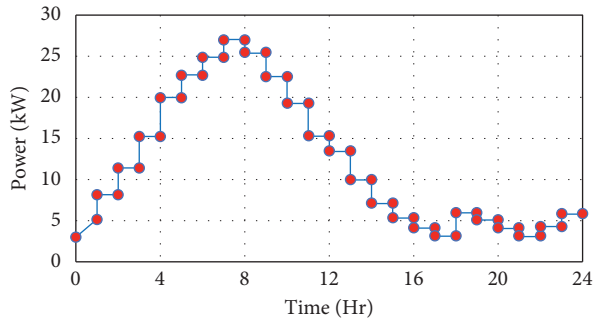


Figure 14: State of charge of the battery—case IV.

of 0.984 kW, and 128.429 kW of power from the other DGs are used and the excess power of 30 kW is transferred to the utility grid during this hour. During the 23rd and 24th hours of the day, based on the utility price and power demand, DGs are operated and power is purchased from the utility to VPP. The excess power generated in the VPP is stored in the storage devices (charging mode). At the end of the day, the SOC of the battery for Case IV is 5.799 kW.

The operating cost (with losses) of VPP for Case IV obtained using the TLBO method is compared with other metaheuristic techniques and is given in Table 13. It is evident from the results that TLBO is superior to other methods as it provides the minimum cost of €ct 797.0170 for without losses and €ct 780.5115 including losses.

The comparison of convergence characteristics for the optimal operating cost for Case IV is illustrated in Figure 15. It is observed that the optimal solution is obtained within 100 iterations when compared to the ABC and ALO methods. From Table 13, it can be observed that the time taken for the convergence of optimal solution using the TLBO algorithm is 7.895 sec, which is lesser than the other methods.

Through the optimal dispatch of power from all the units of VPP using the TLBO algorithm, minimum generation cost is achieved. For the validation of the proposed methodology, four different cases are considered for 2 different test systems and the total generation cost is computed and compared in Table 14. It is evident that, among the three cases for IEEE 16-bus system, Case II is more economical. This is due to the unlimited power exchange option between the VPP and the utility grid, wherein the low utility price during off-peak hours is favorable for VPP to purchase utility power and thereby minimize the generation cost.

Table 13: Comparison of the total cost—Case IV.

| Method | Best solution (€ct) | Worst solution (€ct) | Mean (€ct) | Simulation time (s) |
|---|---|---|---|---|
| Without losses | | | | |
| ABC | 816.1944 | 845.6475 | 817.6637 | 9.987 |
| ALO | 805.5950 | 834.8358 | 806.9115 | 8.158 |
| TLBO | 797.0170 | 827.5376 | 797.5635 | 7.248 |
| With losses | | | | |
| ABC | 799.6889 | 829.1420 | 801.1582 | 10.027 |
| ALO | 789.0895 | 818.3303 | 790.4060 | 8.954 |
| TLBO | 780.5115 | 811.0321 | 781.0580 | 7.895 |

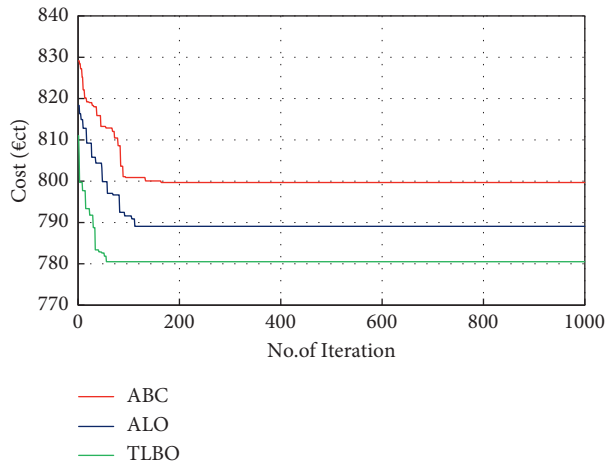


Figure 15: Comparison of convergence characteristics—Case IV.

Table 14: Comparison of the total generation cost—with losses.

| | IEEE 16-bus system | | | IEEE 33-bus system |
|---|---|---|---|---|
| Cases | Case I | Case II | Case III | Case IV |
| Generation cost (€ct) | 758.348 | 735.562 | 751.707 | 780.511 |

In Case I, the maximum power exchange between the utility grid and the VPP is limited to 30 kW. All the units of VPP including RES are in ON state in this case. Therefore, the generation cost is higher than in the other 2 cases. In Case III, the maximum power exchange between the utility grid and the VPP is limited to 30 kW. In addition to that, all the units of VPP are operating in an ON/OFF state based on the corresponding bidding price and start-up/shutdown cost. Therefore, the generation cost is higher than that of Case II. It is observed from the abovementioned case studies that the generation cost of cases with limited power exchange between the utility grid and the VPP is higher compared with the cases with unlimited power exchange. Case II is the most economical and feasible mode of operation. However, in order to reduce the burden on the utility grid and to utilize the maximum available power from the renewable energy sources, Case III is preferable.

## 5. Conclusion

In this paper, the optimal energy management problem of VPP is formulated and implemented using the TLBO algorithm for 24 hours of the day. To evaluate the performance of this optimization algorithm, four different cases are considered. The power is exchanged between the utility grid and the VPP based on their bidding price in all four cases. It is evident from the analysis that the operational cost of VPP is minimized by optimally scheduling the generation of each unit of VPP. It is found that the cases with unlimited power exchange between the utility grid and the VPP is more economical compared to the cases with limited power exchange. Also, Case II is more feasible as it utilized the RES to the maximum extent in spite of the higher bidding price to march towards an emission-free environment. The effectiveness of the TLBO algorithm for this energy management problem is verified in terms of convergence time and

minimum generation cost. As TLBO uses the best solution of the iteration to change the existing solution in the population, convergence rate is improved. It is observed that TLBO gives better performance compared to the other metaheuristic techniques, like ABC and ALO.

## Data Availability

Previously reported data were used to support this study and are cited at relevant places within the text as references [32, 33, 36, 37].

## Conflicts of Interest

The authors declare that they have no conflicts of interest regarding the publication of this paper.

## References


[1] IRENA, *Renewable Energy Capacity Highlights 1st December 2021*, Abu Dhabi, UAE, 2021.

[2] S. M. Nosratabadi, R. A. Hooshmand, and E. Gholipour, "A comprehensive review on microgrid and virtual power plant concepts employed for distributed energy resources scheduling in power systems," *Renewable and Sustainable Energy Reviews*, vol. 67, 2017.

[3] Z. Ullah, G. Mokryani, F. Campean, and Y. F. Hu, "Comprehensive review of VPPs planning, operation and scheduling considering the uncertainties related to renewable energy sources," *IET Energy Systems Integration*, vol. 1, no. 3, pp. 147–157, 2019.

[4] N. Naval and J. M. Yusta, "Virtual power plant models and electricity markets - a review," *Renewable and Sustainable Energy Reviews*, vol. 149, Article ID 111393, 2021.

[5] M. M. Othman, Y. G. Hegazy, and A. Y. Abdelaziz, "A Review of virtual power plant definitions, components, framework and optimization," *International Electrical Engineering Journal*, vol. 6, 2015.

[6] Ł Nikonowicz and J. Milewski, "Virtual Power Plants-general review: structure, application and optimization," *Journal of Power Technologies*, vol. 92, 2012.

[7] P. Moutis, P. S. Georgilakis, and N. D. Hatziargyriou, "Voltage regulation support along a distribution line by a virtual power plant based on a center of mass load modeling," *IEEE Transactions on Smart Grid*, vol. 9, no. 4, pp. 3029–3038, 2018.

[8] R. M. Lima, A. J. Conejo, S. Langodan, I. Hoteit, and O. M. Knio, "Risk-averse formulations and methods for a virtual power plant," *Computers & Operations Research*, vol. 96, pp. 350–373, 2018.

[9] A. Hasankhani and G. B. Gharehpetian, "Virtual power plant management in presence of renewable energy resources," in *Proceedings of the 2016 24th Iranian Conference on Electrical Engineering (ICEE)*, pp. 665–669, IEEE, Shiraz, Iran, May 2016.

[10] L. I. Minchala-Avila, L. E. Garza-Castañón, A. Vargas-Martínez, and Y. Zhang, "A review of optimal control techniques applied to the energy management and control of microgrids," *Procedia Computer Science*, vol. 52, pp. 780–787, 2015.

[11] M. Aien, M. Fotuhi-Firuzabad, and F. Aminifar, "Probabilistic load flow in correlated uncertain environment using unscented transformation," *IEEE Transactions on Power Systems*, vol. 27, no. 4, pp. 2233–2241, 2012.

[12] A. Kavousi-Fard, T. Niknam, and M. Fotuhi-Firuzabad, "Stochastic reconfiguration and optimal coordination of V2G plug-in electric vehicles considering correlated wind power generation," *IEEE Transactions on Sustainable Energy*, vol. 6, no. 3, pp. 822–830, 2015.

[13] T. Geng, L. Xiang, M. Ding, and F. Li, "A bidding model for a virtual power plant via robust optimization approach," *MATEC Web of Conferences*, vol. 95, Article ID 15001, 2017.

[14] Z. Liang and Y. Guo, "Robust optimization based bidding strategy for virtual power plants in electricity markets," in *Proceedings of the 2016 IEEE Power and Energy Society General Meeting (PESGM)*, pp. 1–5, IEEE, Boston, MA, USA, November 2016.

[15] W. Tang and H.-T. Yang, "Optimal operation and bidding strategy of a virtual power plant integrated with energy storage systems and elasticity demand response," *IEEE Access*, vol. 7, pp. 79798–79809, 2019.

[16] Z. Tan, Q. Tan, and Y. Wang, "Bidding strategy of virtual power plant with energy storage power station and photovoltaic and wind power," *Journal of Engineering*, vol. 2018, Article ID 6139086, 11 pages, 2018.

[17] S. Yin, Q. Ai, Z. Li, Y. Zhang, and T. Lu, "Energy management for aggregate prosumers in a virtual power plant: a robust Stackelberg game approach," *International Journal of Electrical Power & Energy Systems*, vol. 117, Article ID 105605, 2020.

[18] A. Baringo, L. Baringo, and J. M. Arroyo, "Day-ahead self-scheduling of a virtual power plant in energy and reserve electricity markets under uncertainty," *IEEE Transactions on Power Systems*, vol. 34, no. 3, pp. 1881–1894, 2019.

[19] D. Dabhi and K. Pandya, "Uncertain scenario based Micro-Grid optimization via hybrid Levy Particle Swarm variable neighborhood search optimization (HL_PS_VNSO)," *IEEE Access*, vol. 8, pp. 108782–108797, 2020.

[20] C. Xiao, D. Sutanto, K. M. Muttaqi, and M. Zhang, "Multi-period data driven control strategy for real-time management of energy storages in virtual power plants integrated with power grid," *International Journal of Electrical Power & Energy Systems*, vol. 118, Article ID 105747, 2020.

[21] O. Erdinc and M. Uzunoglu, "The importance of detailed data utilization on the performance evaluation of a grid-independent hybrid renewable energy system," *International Journal of Hydrogen Energy*, vol. 36, no. 20, pp. 12664–12677, 2011.

[22] M. Vasirani, R. Kota, R. L. G. Cavalcante, S. Ossowski, and N. R. Jennings, "An agent-based approach to virtual power plants of wind power generators and electric vehicles," *IEEE Transactions on Smart Grid*, vol. 4, no. 3, pp. 1314–1322, 2013.

[23] G. Chicco and A. Mazza, "Metaheuristic optimization of power and energy systems: underlying principles and main issues of the 'rush to heuristics," *Energies*, vol. 13, no. 19, p. 5097, 2020.

[24] A. L. Dimeas and N. D. Hatziargyriou, "Agent based control of virtual power plants," in *Proceedings of the 2007 International Conference on Intelligent Systems Applications to Power Systems*, pp. 1–6, IEEE, Kaohsiung, Taiwan, November 2007.

[25] A. de Filippo, M. Lombardi, M. Milano, and A. Borghetti, "Robust optimization for virtual power plants," in *Proceedings of the International Conference of the Italian Association for Artificial Intelligence*, pp. 17–30, Bari, Italy, November 2017.

[26] O. P. Akkas and E. Cam, "Optimal operation of virtual power plant in a day ahead market," in *Proceedings of the 2019 3rd International Symposium on Multidisciplinary Studies and*

*Innovative Technologies (ISMSIT)*, pp. 1–4, IEEE, Ankara, Turkey, October 2019.

[27] Y. Kang, K. Lo, and I. Kockar, "Optimal energy management for virtual power plant with renewable generation," *Energy and Power Engineering*, vol. 09, no. 04, pp. 308–316, 2017.

[28] N. Naval, R. Sánchez, and J. M. Yusta, "A virtual power plant optimal dispatch model with large and small-scale distributed renewable generation," *Renewable Energy*, vol. 151, pp. 57–69, 2020.

[29] M. Shafiekhani, A. Badri, M. Shafie-khah, and J. P. S. Catalão, "Strategic bidding of virtual power plant in energy markets: a bi-level multi-objective approach," *International Journal of Electrical Power & Energy Systems*, vol. 113, pp. 208–219, 2019.

[30] S. Rädle, J. Mast, J. Gerlach, and O. Bringmann, "Computational intelligence based optimization of hierarchical virtual power plants," *Energy Systems*, vol. 12, no. 2, pp. 517–544, 2021.

[31] H. Bai, S. Miao, X. Ran, and C. Ye, "Optimal dispatch strategy of a virtual power plant containing battery switch stations in a unified electricity market," *Energies*, vol. 8, no. 3, pp. 2268–2289, 2015.

[32] A. A. Moghaddam, A. Seifi, T. Niknam, and M. R. Alizadeh Pahlavani, "Multi-objective operation management of a renewable MG (micro-grid) with back-up micro-turbine/fuel cell/battery hybrid power source," *Energy*, vol. 36, no. 11, pp. 6490–6507, 2011.

[33] G. W. Chang, S. Y. Chu, and H. L. Wang, "An improved backward/forward sweep load flow algorithm for radial distribution systems," *IEEE Transactions on Power Systems*, vol. 22, no. 2, pp. 882–884, 2007.

[34] R. V. Rao, V. J. Savsani, and D. P. Vakharia, "Teaching–learning-based optimization: an optimization method for continuous non-linear large scale problems," *Information Sciences*, vol. 183, pp. 1–15, 2012.

[35] G. Waghmare, "Comments on a note on teaching-learning-based optimization algorithm," *Information Sciences*, vol. 229, pp. 159–169, 2013.

[36] A. Baziar and A. Kavousi-Fard, "Considering uncertainty in the optimal energy management of renewable micro-grids including storage devices," *Renewable Energy*, vol. 59, pp. 158–166, 2013.

[37] Z. Wang, B. Chen, J. Wang, M. M. Begovic, and C. Chen, "Coordinated energy management of networked microgrids in distribution systems," *IEEE Transactions on Smart Grid*, vol. 6, no. 1, pp. 45–53, 2015.

[38] S. Papathanassiou, H. Nikos, and S. Kai, "A benchmark low voltage microgrid network," in *Proceedings of the CIGRE Symposium: Power Systems with Dispersed Generation*, Athens, Greece, April 2005.